



Morphological and molecular characterisation of two closely related species: *Myxobolus tihanyensis* n. sp. and *Myxobolus sandrae* Reuss, 1906

Graciela Colunga-Ramírez^{a,b}, Nadhirah Syafiqah Suhaimi^{a,b}, Gábor Cech^a, Kálmán Molnár^a, Csaba Székely^{a,*}, Boglárka Sellyei^a

^a HUN-REN Veterinary Medical Research Institute, Budapest, Hungary

^b Doctoral School of Animal Biotechnology and Animal Science, Hungarian University of Agriculture and Life Sciences, Gödöllő, Hungary

ARTICLE INFO

Keywords:

Cryptic species
Myxobolus tihanyensis n. sp.
Myxobolus sandrae
European perch
Pikeperch
Volga pikeperch

ABSTRACT

Based on spore morphology and small subunit ribosomal DNA sequences, we describe a new *Myxobolus* species, *Myxobolus tihanyensis* n. sp., parasitizing the European perch (*Perca fluviatilis*) from Lake Balaton in Hungary. The brownish plasmodia were found in various locations of the body, mainly in the muscle adjacent with fins and vertebrae. The spores were ovoid, and measured $9.84 \pm 0.38 \mu\text{m}$ in length, $7.69 \pm 0.23 \mu\text{m}$ in width, and $5.35 \pm 0.21 \mu\text{m}$ in thickness, with 8–10 sutural (edge) markings. The polar capsules were mostly equal in size, with $4.91 \pm 0.39 \mu\text{m}$ in length and $2.27 \pm 0.24 \mu\text{m}$ in width. The polar tubule length is $38.15 \mu\text{m} \pm 2.70$, and coiled 6–7 times. In particular, these morphological data overlap with those of *Myxobolus sandrae* Reuss 1906 infecting the European perch (*Perca fluviatilis*), the pikeperch (*Sander lucioperca*), and the Volga pikeperch (*Sander volgensis*) according to previous descriptions and the taxonomic data here described. However, the phylogenetic analyses separate the two species as sister clades with 16.8% genetic distance. This study has demonstrated that the two species of *Myxobolus* exhibit phenotypic similarity while displaying significant genetic divergence. Therefore, the importance of including molecular data in the taxonomic description of myxozoans is emphasized.

1. Introduction

Classifying Myxozoan (phylum Cnidaria) parasites into nominal species provides insights into the estimation of species diversity, ecology, biogeography and their evolution (Brooks and Hoberg, 2000). The genus *Myxobolus* Bütschli, 1882, is one of the most species-rich genera, with more than 900 described members. They are cosmopolitan parasites infecting an extensive diversity of fishes (Liu et al., 2019; Eiras et al., 2021). The validity of their classification is questioned by the occurrence of morphological convergence, as speciation does not necessarily lead to concomitant morphological changes (Bickford et al., 2007; Forró and Eszterbauer, 2016). Several taxonomic descriptions of myxozoans are based only on morphology of the spores, together with biological features such as host specificity and tissue tropism (Molnár and Eszterbauer, 2015). However, most attributes occur as analogous (e. g., length and width measurements), resulting in overlapping features that cause species delimitation difficulties, especially when spores develop in the same organs or tissues of phylogenetically closely related fish hosts (Cech et al., 2012; Holzer et al., 2013; Alama-Bermejo et al.,

2016; Guo et al., 2018). Most myxozoan species are recognised as host-specific and tissue-restricted parasites (Molnár, 1994), while others infect a wide range of hosts regardless of species and type of tissues (Forró and Eszterbauer, 2016). This partial inconsistency leads to a misidentification of species, whereby the authentic diversity of myxozoans is not perceived (Andree et al., 1999; Eszterbauer, 2002; Bartosová-Sojková et al., 2014; Wang et al., 2022). Integrating molecular biology and phylogenetic analyses has significantly accelerated the taxonomic identification of many species, thus effectively resolving the taxonomic challenges (Andree et al., 1999; Guo et al., 2018; Wang et al., 2022).

Currently, several myxozoans belonging to the family Myxobolidae and inhabiting the European perch, *Perca fluviatilis* Linnaeus, 1758, have been identified: *Hennequya psorospermica* Thélohan, 1895, *Hennequya texta* Cohn, 1895, *Hennequya minuta*, Cohn 1896, *Hennequya wolinenis* Romuk-Wodoracki, 1990, *Hennequya dogieli* Akhmerov, 1960, *Hennequya lobosa* and *Hennequya creplini* Gurley, 1894, *Hennequya jaczoi* Székely et al., 2018, *Myxobolus permagnus* Wegener, 1910; *Myxobolus guyenoti* Naville, 1928; and *Myxobolus sandrae* Reuss (1906); Lom et al.

* Corresponding author.

E-mail address: szekely.csaba@vmri.hun-ren.hu (C. Székely).

<https://doi.org/10.1016/j.ijppaw.2024.100909>

Received 22 December 2023; Received in revised form 23 January 2024; Accepted 23 January 2024

Available online 5 February 2024

2213-2244/© 2024 The Authors. Published by Elsevier Ltd on behalf of Australian Society for Parasitology. This is an open access article under the CC BY-NC-ND license (<http://creativecommons.org/licenses/by-nc-nd/4.0/>).

(1991); Székely et al. (2018). The species mentioned above create plasmodia in gills, except *H. wolinensis* – epidermis under the scales, and *M. sandrae*. The latter was detected in the muscles and intermuscular connective tissue outside the vertebral column and was described as a pathogen causing severe damage to the caudal nerves and abnormal curvature of the vertebral column of the European perch (Lom et al., 1991). Originally, *M. sandrae* was described from the muscles of the pikeperch, *Sander lucioperca* (Linnaeus, 1758) by Reuss (1906) and later documented by Soltyńska (1967). Subsequently, Andree et al. (1999) and Ferguson et al. (2008) also provided 18 S rDNA gene sequences without morphological data. In the routine parasitological survey of the European perch collected in Lake Balaton, we detected plasmodia in the musculature near the skin covered base of the fin rays, in and in the vicinity of the vertebral column and the buccal cavity. Interestingly, according to spore morphology, the *Myxobolus* spores presented here were remarkably similar to *M. sandrae* (Lom et al., 1991).

Therefore, in order to clarify the contradictions and establish the validity of *Myxobolus tihanyensis* n. sp. as a novel species, morphological and molecular data were performed and compared with the existing descriptions of *M. sandrae*, including updated information on spore morphology and molecular data.

2. Material and methods

2.1. Sample collection

Perca fluviatilis specimens (n = 23; total length 8–13 cm) were collected in March 2023 in Tihany, Lake Balaton (46.90891° N, 17.87923° E). All specimens were transported alive in oxygenated plastic containers to the Laboratory of Fish Pathology and Parasitology at the Veterinary Medical Research Institute (HUN-REN VMRI) and kept in an aerated aquarium until necropsy. The perch were routinely screened for myxozoan parasites by macroscopic examination. All procedures were performed in accordance with the European Directive on the Protection of Animals Used for Scientific Purposes (Directive, 2010/63/EU). Therefore, specimens were anaesthetised and slaughtered by a cervical cut. All organs, including the skeleton (head, trunk, and fins), were removed and observed under a stereo-microscope (Olympus SZX16) for plasmodia detection. If plasmodia were present, photomicrographs were taken under a light microscope (Olympus BX53) equipped with a digital camera (Olympus DP74). Subsequently, the plasmodia were ruptured by a sharp needle, and the spores were collected in 1.5 ml microcentrifuge tubes filled with 80% ethanol for morphological and molecular analyses (Sellyei et al., 2022). Similarly, sample stocks of *Myxobolus sandrae* were processed from infected muscles of *Sander lucioperca* (n = 3) and *Sander volgensis* (Gmelin, 1789) (n = 1) collected in Lake Balaton in 1996 and 2005, respectively, and stored at –20 °C in the Fish Pathology and Parasitology Laboratory at the Veterinary Medical Research Institute (HUN-REN VMRI).

2.2. Morphological identification

Fresh and Lugol-stained spores were mounted on glass slides under a coverslip and measured according to the guidelines of Lom and Arthur (1989) using ImageJ software (<http://imagej.nih.gov/ij>).

For histology, the posterior part of the body with the caudal fin of two infected perches was used, cutting them in sagittal or transverse directions, respectively. The sagittal section was fixed in Bouin's solution for 4 h. The transversal section – was fixed in 10% formalin for 3 days, then soaked in 5% HCL for 5 h. Both the samples were washed and dehydrated in an ascending ethanol series and embedded in paraffin wax. In addition, the paraffin block with transversal section was decalcified in RDC (Rapid Decalcifier, HLJ-011, Histo-Lab) solution for 3 h and washed under running water for 30 min to remove the solution. The blocks were then cut into 4–5 µm sections and stained with haematoxylin and eosin (H&E).

Photomicrographs about histological slides were taken under a light microscope (Olympus BX53) with a digital camera (Olympus DP74). All measurements are given in micrometres (µm) and are presented as the mean, followed by the ±standard deviation (SD) and the range in parentheses.

2.3. PCR and sequencing

DNA was extracted from myxosporean spores isolated from perch, pikeperch, and Volga pikeperch using a Genomic DNA Mini Kit (Geneaid Biotech Ltd., Taiwan) according to the manufacturer's instructions. Two overlapping fragments of the 18 S ribosomal RNA (18 S rDNA) gene were amplified by Polymerase chain reaction (PCR) using the following primer pairs: ACT1F-ACT1R, and Myxgen4F-Myxgen4R, and Myxgen4F-ERB10 (Barta et al., 1997; Hallett and Diamant 2001; Diamant et al., 2004) (see Table 1 for more details). Primers amplified three overlapping fragments from 600 to 900 bp, approximately. All PCR amplifications were performed in 50 µl volume reactions using 5 µl of 10 × DreamTaq buffer (Thermo Scientific, Vilnius, Lithuania), 1 µl of 2 mM dNTP mix (Thermo Scientific), 0.5 µl of 10 pmol of each primer, 0.5 µl of DreamTaq polymerase (1 U; Thermo Scientific), 1 µl of template DNA, and 41.5 µl of nuclease-free water to volume. The amplification conditions were the same for all paired primers: 94 °C for 3 min, followed by 35 cycles of three steps of 94 °C for 45 s, 55 °C for 50 s, and 72 °C for 1 min; and a final elongation step of 72 °C for 10 min. DNA amplicons were electrophoresed through a 1% agarose 1 × tris-acetate-EDTA buffer (TAE) gel stained with ethidium bromide (0.5 µl/ml) and examined under ultraviolet light. The appropriate-sized bands were cleaned with the DNA Fragment Purification Kit (Invitex, Berlin, Germany). Each PCR product was sequenced with the same primers performed for amplification in both (forward and reverse) directions using a BigDye Terminator v3.1 Cycle Sequencing Kit (Applied Biosystems, Foster City, USA) and run on an ABI PRISM 3100 Genetic Analyser (Applied Biosystems).

2.4. Phylogenetic analyses

The sequence chromatograms were checked visually and edited in Chromas software v. 2.6.6 and assembled in MEGA 11 (Tamura et al., 2021). To determine the phylogenetic relationship, 32 representative sequences of the 18 S rDNA gene of myxosporeans were retrieved from the GenBank database (see Appendix S1 for more details), and the *Chloromyxum auratum* (AY971521) sequence was used as an outgroup. The nucleotide sequences were aligned using ClustalW in MEGA 11 (Tamura et al., 2021), and ambiguously aligned positions were eliminated using GBLOCKS v0.91 b with less stringent selection parameters (Castresana, 2000; Talavera and Castresana, 2007).

Phylogenetic relationships were performed using Maximum Likelihood (ML) and Bayesian Inference (BI). Both analyses were performed using the general time-reversible model (GTR + G) as the most plausible

Table 1

List of primers used for the amplification and sequencing of the 18 S rDNA gene for *Myxobolus tihanyensis* n. sp. and *Myxobolus sandrae*.

Primer	Sequence (5'–3')	Paired with	Reference
ACT1F (forward)	TGGCAGCGAGAGGTGAAATT	ACT1R	Hallett and Diamant (2001)
ACT1R (reverse)	AATTTACCTCTCGCTGCCA	ACT1F	Hallett and Diamant (2001)
Myxgen4F (forward)	GTGCCTTGAATAAATCAGAG	Myxgen4R	Diamant et al. (2004)
Myxgen4R (reverse)	CTY TGATTATTCAAGGCAC	Myxgen4F	Diamant et al. (2004)
ERB10 (reverse)	CTCCGCAGGTTCCACCTACGG	Myxgen4F	Barta et al. (1997)

model according to the Akaike Information Criterion (AIC) and Bayesian Information Criterion (BIC) executed in jModelTest 2.1.10 v20160303 (Darriba et al., 2012). ML analyses were performed by MEGA 11 (Tamura et al., 2021), and nodal support values were calculated based on Bootstrap analysis using 1000 replicates. Similarly, BI analyses were conducted by MrBayes v. 3.2 (Ronquist et al., 2012), using $nst = 6$, with gamma-distributed rate variation across sites and a proportion of invariable sites (rates = invgamma). Posterior probability distributions were generated using the Markov Chain Monte Carlo (MCMC) method, with four chains running simultaneously for 2,000,000 generations. Burn-in was set at 2,500, and trees were sampled every 100 generations, making a total of 7500 trees used to compile the majority rule consensus trees. Bootstrap values (BS) $\geq 70\%$ for ML and Posterior probabilities (PP) ≥ 0.95 values for BI analyses were considered strongly supportive for clades. The resulting trees were first visualised in MEGA 11 (Tamura et al., 2021) and FigTree v. 1.4.4 (Rambaut, 2018), respectively, and both were edited in CorelDRAW Graphics Suite 2019 v. 21.3.0.755. To evaluate the genetic distance between the *Myxobolus* species clustering together with the newly obtained sequences, the pairwise method with the *p*-distance model was carried out in MEGA 11. The variance was estimated by the bootstrap method (1000 replicates) and the uniform nucleotide substitution rate (transition + transversions).

3. Results

All ($n = 21$) examined specimens of *P. fluviatilis* were infected by spore-forming plasmodia associated with the connective tissue in different fish body regions, mentioned below: attached to the subcutaneous muscle beneath the hypodermis (Fig. 1C and Supplementary Fig. S1B), adjacent to the vertebral skeletal system, close to the neural and hemal spines (Fig. 4C–D and Supplementary Fig. S1A) under the skin among the rays (interrays) near the distal radials of the pectoral and

pelvic fins (Supplementary Figs. S1C–D), or close to the proximal radials (pterygiophore) of the dorsal and anal fins; associated with the hypural plates of the caudal fin (homocercal tails) (Fig. 1B–D) and Supplementary Fig. E), and the cartilaginous palatal region of the buccal cavity (Supplementary Fig. S1G).

In the rest of the fish body, plasmodia of *Myxobolus tihanyensis* n. sp. were not detected. Furthermore, the fish showed no abnormalities, such as lesions or deformities related to this parasite. Morphometric, morphological, and molecular analyses (Figs. 1–5) indicated that the myxosporean collected in Tihany on Lake Balaton, should be considered a new species of the genus *Myxobolus*.

3.1. Description

3.1.1. *Myxobolus tihanyensis* n. sp.

Plasmodia ($n = 50$): brownish and polymorphic in (long, slender, spherical to ovoid) shape; and vary in size, $249 \mu\text{m} \pm 156$ (60–850) length, $174 \mu\text{m} \pm 49$ (50–523). Rarely irregularly shaped plasmodia ($n = 2$) were recorded (Fig. 1; Fig. S1). However, all examined plasmodia contained mature spores.

Spores ($n = 30$): Mature spores are ovoid or slightly pyriform in shape (Figs. 2 and 3). The sutural ridge presents 8–10 sutural markings symmetrically distributed. Spore length $9.74 \mu\text{m} \pm 0.33$ (8.6–10.19). Width $7.69 \mu\text{m} \pm 0.23$ (7.2–8.15) and thickness $5.35 \mu\text{m} \pm 0.21$ (5.08–5.78) (Fig. 2, Table 2). Spores with 2 polar capsules of approximately equal size, length $4.9 \mu\text{m} \pm 0.39$ (4.05–5.87), width $2.27 \mu\text{m} \pm 0.24$ (1.78–2.75) (Fig. 2B–F). Polar tubule coiled 6–7 times, with a length of $38.15 \mu\text{m} \pm 2.70$ (32.36–42.61) (Fig. 2D–H). All spore measurements were taken on fresh spores, with the exception of the polar tubule length, measured after Lugol staining.

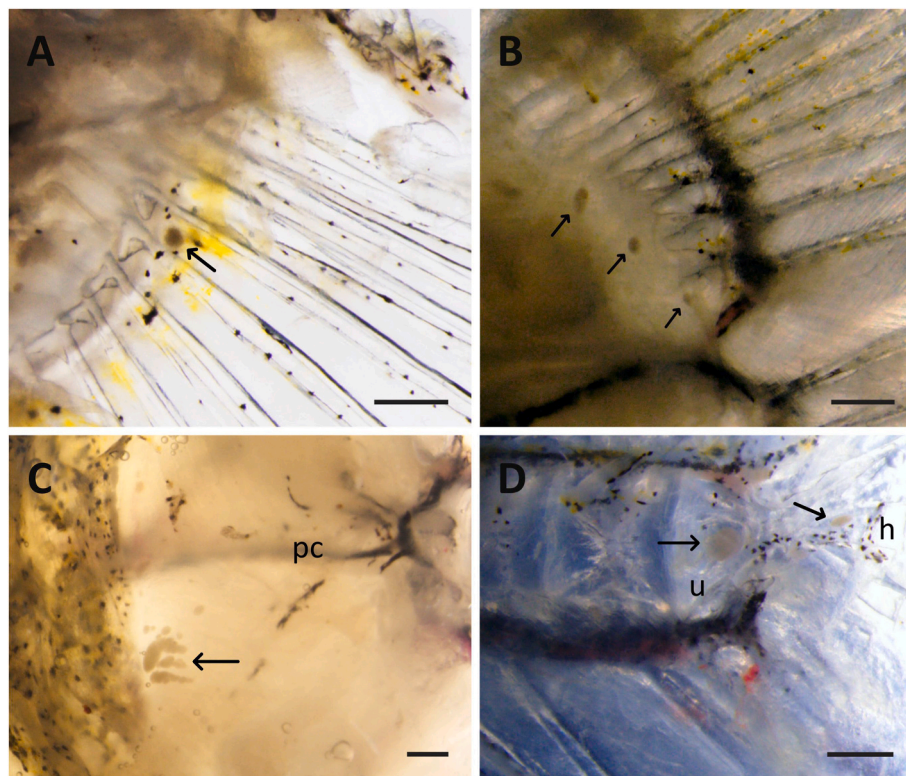


Fig. 1. *Myxobolus tihanyensis* n. sp. plasmodia inhabiting *Perca fluviatilis*. (A) Plasmodia in the mesenchymal tissue between the caudal fin rays beneath the skin. (B) Plasmodia in the subcutaneous muscle close to the cartilage and ossified caudal fin rays (C) Plasmodia close to the pleural centrum (pc) located in the homocercal caudal fin. (D) Plasmodia is shown in the homocercal caudal skeleton in the urostyle (u) and the hypural (h). Note plasmodia are indicated in black arrows. Scale bars = 500 μm .

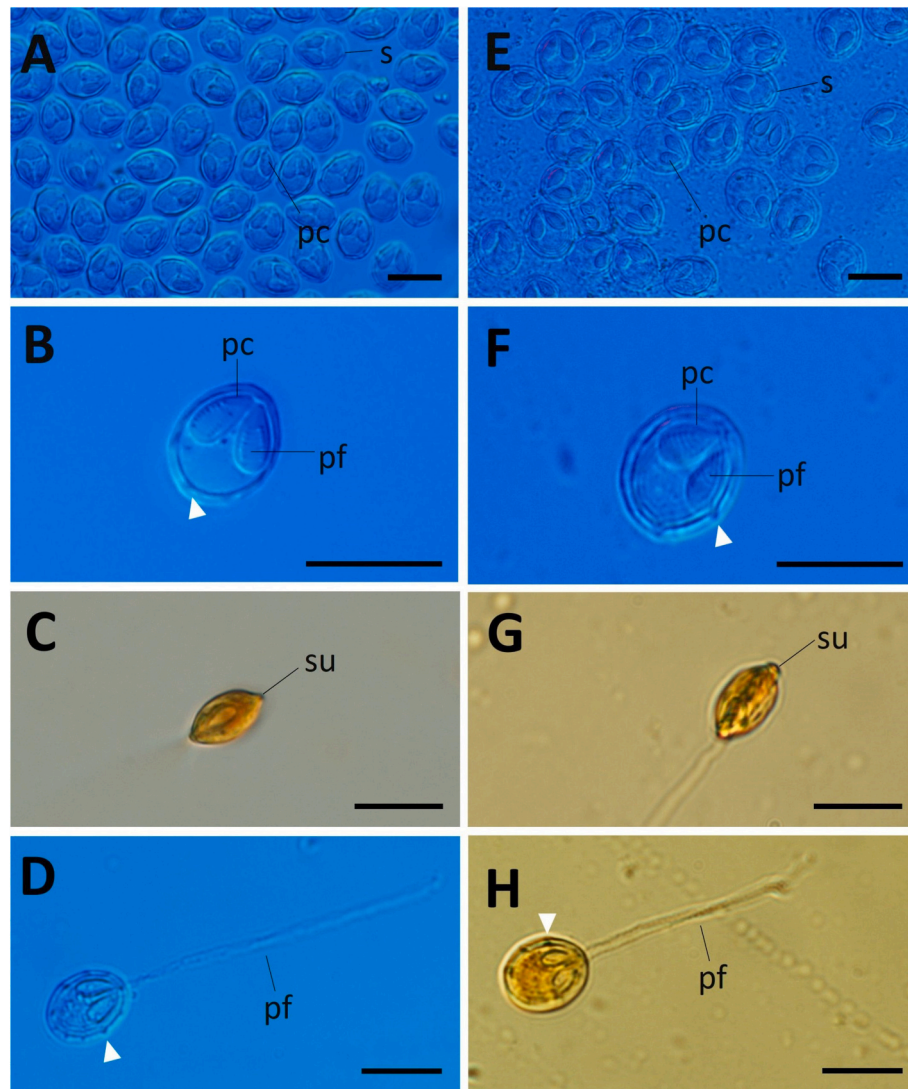


Fig. 2. Photomicrographs of *Myxobolus tihanyensis* n. sp. spores from *Perca fluviatilis*. (A–D) *Myxobolus tihanyensis* n. sp., and (E–H), *Myxobolus sandrae* from *Sander lucioperca*. (A, E) Numerous mature spores (s) illustrate an ovoid shape and two polar capsules (pc). (B, F) Ovoid spores with sutural markings (white arrows) with two polar capsules which contain coiled polar tubules (pf) (C, G) Spore in sutural view showing the suture (su) (D, H) Spores releasing the polar tubules (pf) and showing sutural markings. Figs. C, G and H represented spores stained with Lugol solution. Scale bars = 10 μ m.

3.2. Taxonomy summary

Type host: *Perca fluviatilis* Linnaeus, 1758, European perch (Percidae).

Locality: Tihany, Lake Balaton, Hungary (46.90891° N, 17.87923° E).

Prevalence of infection: 21/21 (100%)

Infection site: Spore-forming plasmodia located predominantly at the fin bases adjacent to radials as follows: caudal fin 23/23 (100%), anal fin 3/23 (13%), anterior and posterior dorsal fin 8/23 (34.7%), pectoral fins 7/23 (30.4%), pelvic fins 8/23 (34.7%). Some were found between the hemal and/or neural spines and muscle fibers 3/23 (13%), but also in the muscles attached to the vertebrae of the spine 7/23 (30.4%), and occasionally in the cartilage palatal region of the buccal cavity 2/23 (8.6%). No plasmodia were found in the trunk muscle.

Histology: Small, round, oval or amorphous plasmodia of *Myxobolus tihanyensis* n. sp. were observed in the connective tissue, namely in the lepidotrichial region between the fin rays or near the proximal pterygiophores of the fins (Fig. 4A–BA), and between the hemal spines and muscle fibers (Fig. 4C–D). Despite severe infection with plasmodia in the hypural region of the caudal fin, no discernible morphological changes

or observable lesions were detected.

Sequences: 18 S rDNA sequences were deposited in the GenBank under the accession numbers OR960700, OR960701, OR960702, OR960703, OR960704.

Type material: Photo-types and histological preparations were deposited in the parasitological collection of the Zoological Department, Hungarian Natural History Museum, Budapest, Coll. No. HNHM-PAR-20893.

Etymology: The name of the species refers to the name of the town of Tihany, where the first host specimens were collected from Lake Balaton.

Remarks: The myxospores of *Myxobolus tihanyensis* n. sp. overlap morphometrically and morphologically with *M. sandrae*. The comparative metrical data and microphotographs of the present species and *M. sandrae* are provided in Table 2 and Fig. 2, respectively. BLAST analysis of the 18 S rDNA gene sequences revealed no significant similarity ($\leq 89\%$) with any known myxosporean species. The molecular phylogenetic analyses confirm that *Myxobolus tihanyensis* n. sp. was robustly placed in a monophyletic group that exhibited the closest genetic relationship with *M. sandrae* (Fig. 5).

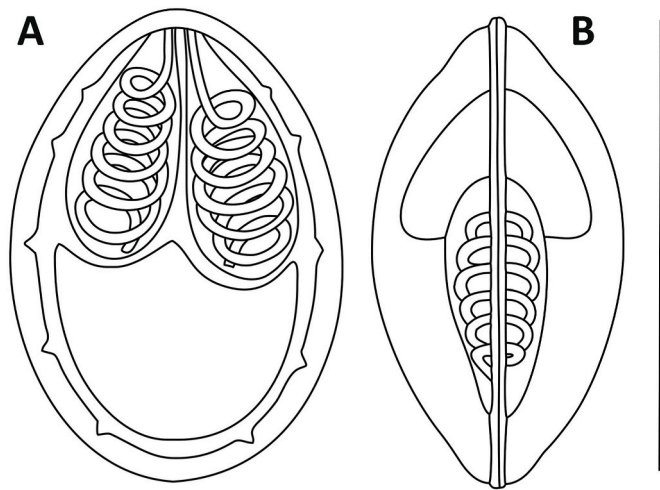


Fig. 3. Schematic drawings of the mature spore of *Myxobolus tihanyensis* n. sp. from the caudal fin of *Perca fluviatilis* (A) in frontal view, (B) in sutural view. Scale bar = 10 μ m.

3.3. Phylogenetic analyses

Five partial 18 S rDNA sequences of *Myxobolus tihanyensis* n. sp. (in a total length of 1584 bp, 1596 bp, 1591 bp, 1595 bp, 1579 bp with their respective GenBank accession number OR960700, OR960701, OR960702, OR960703, OR960704) obtained from five European perch, four *M. sandrae* sequences from three pikeperch, and one *Volga pikeperch* (in a total length of 1567 bp, 1564 bp, 1561 bp, 1553 bp with their respective GenBank accession numbers: OR951403, OR951404,

OR951405, OR951404) were compared with each other and other myxozoan sequences. Each sequence of *Myxobolus tihanyensis* n. sp. from different body regions (e.g., caudal fin, dorsal fin, vertebrae, and buccal cavity) confirmed that all spore-forming plasmodia belonged to the same species.

The final dataset comprised a total of 42 taxa and 1151 positions, and the phylogenetic analyses revealed analogous ML and BI topologies. Therefore, only the BI tree was used to represent the general tree topology (Fig. 5; Supplementary Fig. S2). All sequences of *Myxobolus tihanyensis* n. sp. were grouped in the same clade and were conspecific with the highest nodal support values (PP = 1.0 and BS = 100%). This clade formed a sister group to another well-supported monophyletic clade (PP = 1.0 and BS \geq 86%), which included both the *M. sandrae* sequences from the present study and those of Ferguson et al. (2008) (PP = 1.0 and BS = 100%) (Fig. 5). The genetic divergence values between *Myxobolus tihanyensis* n. sp. and *M. sandrae* (EU346379) and *M. sandrae* (AF085181) were 16.8%, and 27.7%, respectively. In contrast, the divergence distance between both *M. sandrae* sequences (AF085181 and EU346379) was 30.3%. The difference varied from 16.3% to 18.3% between *Myxobolus tihanyensis* n. sp. and other *Myxobolus* species. (Table 3).

4. Discussion

The present study was conducted to identify *Myxobolus tihanyensis* n. sp. inhabiting the European perch based on morphological features, phylogenetic analyses, and genetic distance. Our results provide evidence for the discovery of a novel species of *Myxobolus*. Furthermore, our findings demonstrated that spores of *M. tihanyensis* n. sp. and *M. sandrae*, previously recorded by Reuss (1906), Soltyska (1967) and Lom et al. (1991), could not be distinguished by morphological

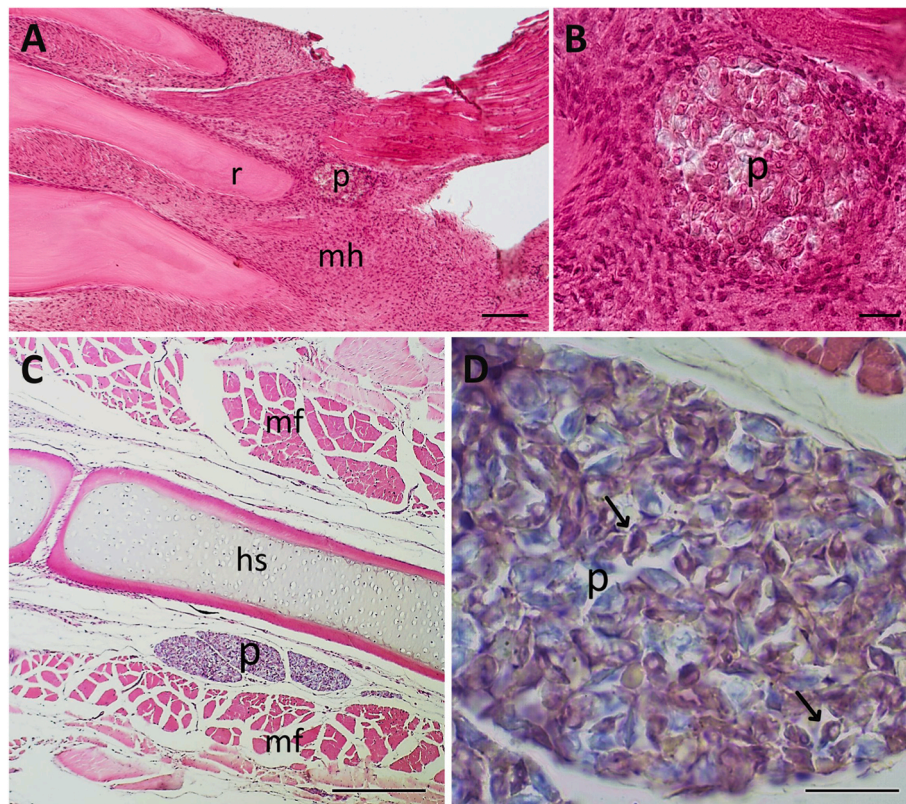


Fig. 4. Histology sections of *Perca fluviatilis* using the haematoxylin and eosin (H & E) technique. (A–B) Sagittal section of the proximal region of the caudal fin. (A) Rounded plasmodia (p) developing in the mesenchyme (mh) closely attached to the bases of the rays (r), scale bar = 100 μ m. (B) Higher magnification of plasmodia-containing spores. Scale bar = 20 μ m. (C–D) Transversal section of the caudal vertebrae region. (C) Plasmodia located between the hemal spine (hs) and muscular fibres (mf), scale bar = 200 μ m. (D) Higher magnification of plasmodia containing spores (black arrows), scale bar = 20 μ m.

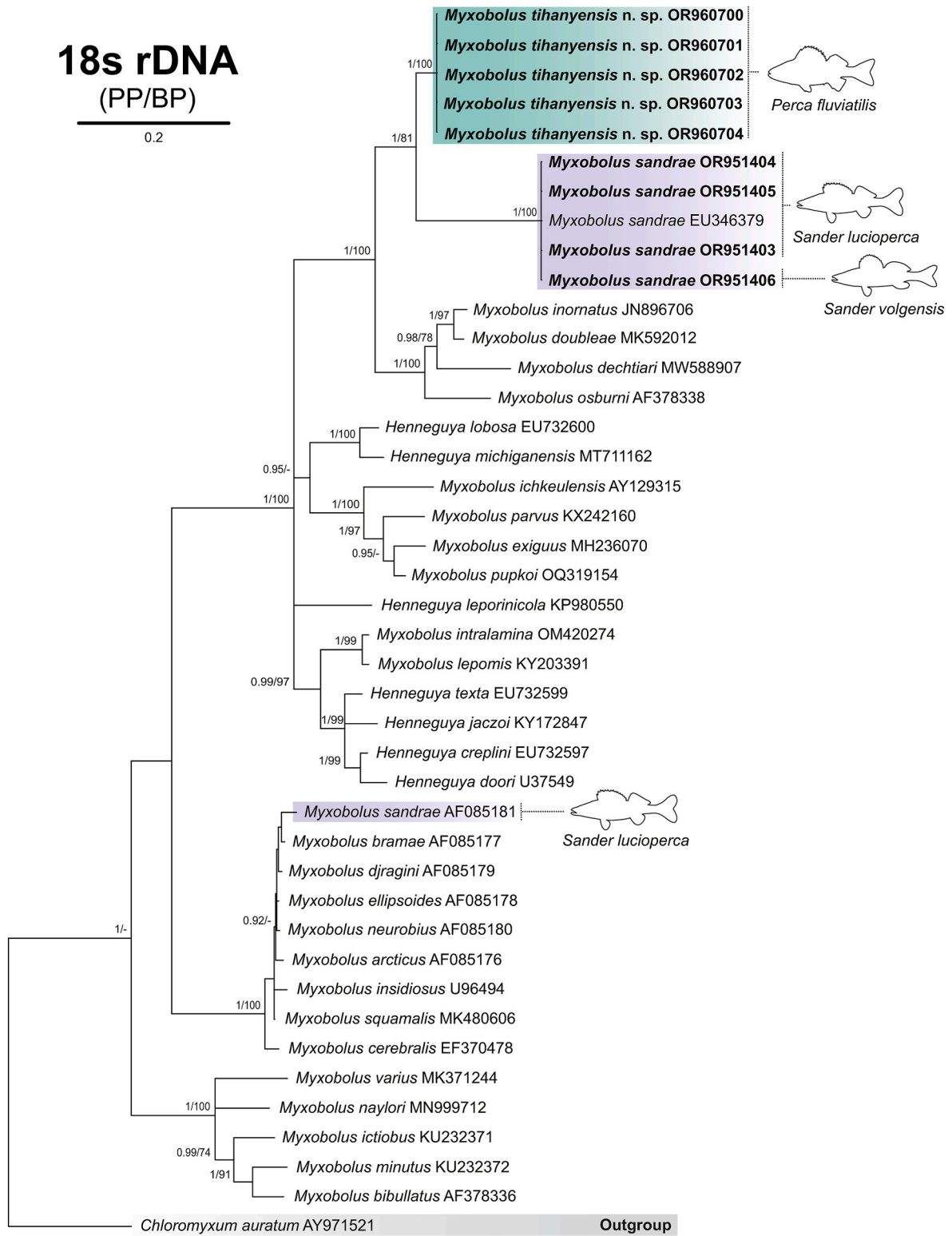


Fig. 5. Bayesian inference phylogenetic tree based on dataset of 42 aligned myxosporean 18 S rDNA sequences. The GenBank accession numbers are shown next to the species names. *Chloromyxum auratum* was used as an outgroup. Posterior probabilities (PP)/maximum likelihood bootstrap (BS) values are shown above the nodes. Weakly supported nodes (PP < 0.95 and BS < 70%) are represented with dashes or blanks. Scale bar = 0.2 substitutions per site. Note: The fish host species names of *Myxobolus tihanyensis* n. sp. and *Myxobolus sandrae* are indicated under their drawings. The complete data of all sequences used in this analysis are listed in the [Supplementary Table S1](#).

Table 2

Comparative description of *Myxobolus tihanyensis* n. sp. with morphologically similar species, including *Myxobolus sandrae*. Mean \pm SD and range in parentheses are expressed in μm . Unavailable data are indicated by a dash (–).

<i>Myxobolus</i> spp.	Shape	Spore length	Spore width	Thickness	Polar capsule length	Polar capsule width	Polar filament coiled	Polar filament length	Sutural markings	Infection site	Host	Reference
<i>M. tihanyensis</i> n. sp.	Ovoid	9.84 \pm 0.38 (8.67–10.85)	7.69 \pm 0.23 (7.28–8.15)	5.35 \pm 0.21 (5.08–5.78)	4.91 \pm 0.39 (4.05–5.87)	2.27 \pm 0.24 (1.78–2.75)	6–8	38.15 \pm 2.70 (32.36–42.61)	8–10	Muscle and subcutaneous muscle near the fins, vertebrates. Cartilage of the buccal cavity	<i>Perca fluviatilis</i>	This study
<i>M. sandrae</i>	Discoidal, ovoid	10.26 \pm 0.40 (9.4–11.3)	8.5 \pm 0.36 (7.6–9.2)	5.50 \pm 0.34 (4.83–6.12)	4.60 (3.7–5.2)	2.40 (1.79–2.89)	6–8	32.25 \pm 3 (27.97–77.35)	8–10	Muscle	<i>Sander lucioperca</i> and <i>Sander volgensis</i>	This study
<i>M. sandrae</i>	Ellipsoidal	10.1 (9.2–11.3)	8.0 (7.4–8.5)	NA	–	–	6	NA	6	Muscles and intermuscular connective tissues outside of the vertebral column	<i>Perca fluviatilis</i>	Lom et al. (1991)
<i>M. sandrae</i>	Oval, discoidal, ovoid	6.8–10.6	5.7–8.5	3.8–6	3.2–5.4	1.3–2.7	7–8	30–35	5–8	Connective tissue of the head, branchial, cavity, gills	<i>Sander lucioperca</i>	Soltyńska (1967)
<i>M. sandrae</i>	Ovioid	9.25 (9.25–10)	7.75 (7.25–8.26)	NA	3.5 (3.5–4)	2 (1.16–2.2)	–	–	–	Muscle	<i>Sander lucioperca</i>	Reuss (1906)
<i>M. inornatus</i>	Ovoid, pyriform	11.3 \pm 0.2 (8.6–17.4)	8.6 \pm 0 (7.1–13.7)	6.6 \pm 0.1 (5.7–7.8)	5.6 \pm 0.2 (4.2–9.5)	2.6 \pm 0.1 (1.7–4.6)	6–8	21.7 \pm 0.9 22 (17.2–27.2)	8–10	Muscle	<i>Micropterus dolomieu</i>	Walsh et al. (2012)
<i>M. doubleae</i>	Rounded	11.7 \pm 0.4 (10.7–12.3)	8.6 \pm 0.4 (7.7–9.0)	5.2 \pm 0.4 (4.6–5.6)	5.7 \pm 0.4 (5.1–6.5)	2.7 \pm 0.2 (2.4–3.2)	8–9	50	Yes	Intrafilamental-epithelial gills	<i>Perca flavescens</i>	Milanin et al. (2020)
<i>M. osburni</i>	Ovoid	10.15 (9.6–11.2)	11.79 (9.6–12.8)	6.8 (6.4–8.0)	5.2 (4.8–5.6)	NA	6–7	35.2 (30.4–40)	10	Mesentary	<i>Micropterus dolomieu</i> and <i>Eupomotis gibbosus</i>	Herrick (1936)
<i>M. dechtiari</i>	Ovoid	11.5 (10.0–14.0)	8.0 (7.0–9.0)	7.5 (7.0–8.0)	5.0 (4.0–6.0)	2.5 (2.0–3.0)	–	44 (37–55)	7–9	Gills	<i>Lepomis gibbosus</i>	Cone and Anderson (1977)

Table 3

Genetic *p*-distance (below the diagonal) and sequence similarities (in %, above the diagonal) of *Myxobolus tihanyensis* n. sp., *Myxobolus sandrae*, and closely related *Myxobolus* spp. based on 18 S rDNA sequence data, followed by their respective GenBank accession numbers.

	1	2	3	4	5	6	7	8
1. <i>Myxobolus tihanyensis</i> n. sp. (OR960700–4)		83.2	83.2	72.3	83.7	83.6	83.1	81.7
2. <i>Myxobolus sandrae</i> (OR951403–6)	0.168		100	69.7	79.1	79.4	78.8	77.4
3. <i>Myxobolus sandrae</i> (EU346379)	0.168	0.000		69.7	79.1	79.4	78.8	77.4
4. <i>Myxobolus sandrae</i> (AF085181)	0.277	0.303	0.303		71.3	72.5	72.2	71.5
5. <i>Myxobolus inornatus</i> (JN8967069)	0.163	0.209	0.209	0.287		95.7	85.3	87.1
6. <i>Myxobolus doubleae</i> (MK592012)	0.164	0.206	0.206	0.275	0.043		85.7	86.9
7. <i>Myxobolus osburni</i> (AF378338)	0.169	0.212	0.212	0.278	0.147	0.143		83.9
8. <i>Myxobolus dechtiari</i> (MW588907)	0.183	0.226	0.226	0.285	0.129	0.131	0.161	

comparisons; however, it is possible to separate these two species by molecular analysis. The taxa *M. tihanyensis* n. sp. and *M. sandrae* exhibit unambiguous divergence from a shared ancestral lineage and are distinctly classified into sister clades, supported by evidence of genetic distance. Therefore, it is clear that without genetic data, it would have been impossible to distinguish and identify this new species based merely on morphology and host species information.

Andree et al. (1999) were the first to compare the 18 S rDNA sequences of several *Myxobolus* species. They found a low correlation between spore morphology and size or host specificity. However, in some cases, spores of similar size and shape (e.g., *Myxobolus cerebralis* Hofer, 1903 and *Myxobolus squamalis* Iversen, 1954) were phylogenetically distant from each other. In contrast, spores with divergent morphology and size were sometimes found to be closely related (e.g., *M. cerebralis* and *Myxobolus insidiosus* Wyatt and Pratt, 1963). In this context, the myxozoans demonstrated the limitations of taxonomy based on the size and morphological characteristics of spores and host species; and strongly recommended the inclusion of molecular data in taxonomic analyses. The study of Andree et al. (1999) provided molecular data for the identification of some myxozoans without morphometric information. Comparing molecular data of *M. tihanyensis* n. sp. with the *M. sandrae* sequences (AF085181 by Andree et al. (1999) and EU346379 by Ferguson et al. (2008)) indicated 72.3% similarity (27.7% genetic distance) and 83.2% similarity with 30.3% genetic distance, respectively (Table 3). Meanwhile, Ferguson et al. (2008) reported a 65.9% genetic similarity percentage between sample sequences AF085181 and EU346379; we reported 69.7% similarity. The *M. sandrae* sequences here generated (OR951403–6) are identical to *M. sandrae* of Ferguson et al. (2008). Furthermore, our results indicate a higher percentage of sequence similarity (83.2%) between the sequences of *M. tihanyensis* n. sp. with the sequence here provided of *M. sandrae* and EU346379 (Table 3). Comparing our results with the phylogenetic tree of Andree et al. (1999) a similar clade topology can be observed. Where the *M. sandrae* sequence (AF085181) is positioned in a clade comprising *Myxobolus bramae* Reuss (1906), *Myxobolus djragini* (Akhmerov, 1954), *Myxobolus ellipsoides* Thélohan, 1892, *Myxobolus neurobius* Schuberg and Schroder, 1905, *Myxobolus arcticus* Pugachev and Khokhlov, 1979, *Myxobolus insidiosus* Wyatt and Pratt, 1963, and *Myxobolus squamalis* (Iversen, 1954); and rooted in another clade comprised of *M. cerebralis*. Against this background and in the absence of morphological data for the sequence AF085181, the identification of the specimen as *M. sandrae* is questionable; that the record AF085181 could correspond to a still undescribed species (Ferguson et al., 2008).

The morphological descriptions of *M. sandrae*, a muscle-dwelling parasite of pikeperch, were primarily reported via line drawings. Then, a further insight was presented by Lom et al. (1991), providing microphotographs of fresh spores. However, it is important to note that the samples in the latter publication, by Lom et al. (1991), were collected from a different species of fish, namely the European perch, particularly from the intermuscular connective tissue near the vertebrae. Compared to the previous descriptions, our microphotographs reveal that the spores of *M. sandrae* have a somewhat rounder shape.

Although morphological and molecular genetic investigations are

preferred, studying host, organ, and tissue specificity provides additional important information for accurately identifying myxosporean spp. Molnár (1994) found that most myxosporeans have a relatively strict organ specificity and an even stricter tissue specificity. Investigating this issue, Molnár and Székely (2014) demonstrated that *M. sandrae*, a known parasite of the musculature of the pikeperch, should be considered a parasite of connective tissue, as its vegetative development and sporogony occur in the intermuscular connective tissue. The plasmodia and spores of *M. tihanyensis* n. sp. showed morphological similarity with *M. sandrae* and were also closely related in their molecular sequences.

In its histology, the new species also proved to be connective tissue-specific. However, the two species differed regarding host and location in organs. While plasmodia of *M. sandrae* are mainly associated with the connective tissue of the skeletal muscle, the plasmodia of *M. tihanyensis* n. sp. develop near the basal part of fins and close to the vertebral column. In contrast, *M. sandrae* from European perch (described by Lom et al., 1991) resembles *M. tihanyensis* n. sp. not only in morphology but host fish, and tissue tropisms (vicinity of the vertebral column) implying a potential close relationship between them.

The concept of cryptic species has been earning a fast reputation in myxozoan descriptions. Cryptic species can be defined as two or more morphologically indistinguishable species that can be differentiated solely via molecular analyses (Sáez and Lozano, 2005; Bickford et al., 2007). Among the myxobolids, some species have been identified as potentially cryptic (Ferguson et al., 2008; Cech et al., 2012; Atkinson et al., 2015; Vieira et al., 2022). For example, based on the morphological similarities observed among *Myxobolus* gill infections in cyprinids, it is possible to infer that the ide (*Leuciscus idus* Linnaeus, 1758), asp (*Aspius aspius* Linnaeus, 1758), and white bream (*Blicca bjoerkna* Linnaeus, 1758) may be susceptible to infection by *Myxobolus dujardini*, which was previously described in chub (*Leuciscus cephalus* Linnaeus, 1758). However, the 18 S rDNA sequence analysis of the spores revealed there are two different species: *Myxobolus alvarezae* Cech et al., 2012 which parasite two fish species, namely the ide and asp; and *Myxobolus sitjae* Cech et al., 2012 infesting white bream, are involved in these infections (Cech et al., 2012). Concurrently, it has been hypothesized that closely related host species tend to have more similar parasites, and phylogenetically more similar parasite species tend to infect a phylogenetically similar group of host species (Dallas and Becker, 2021). In this regard, the European perch (*P. fluviatilis*), the pikeperch (*S. lucio-perca*), and the Volga pikeperch (*S. volgensis*) belong to the same family (Percidae), they are morphologically very similar and their geographical distribution overlapping in Europe, including Lake Balaton in Hungary (Specziár and Bíró, 2003; Kottelat and Freyhof, 2007; Weiperth, 2014). The morphological and molecular findings presented in this study confirm that *M. sandrae* also inhabits Volga pikeperch, in agreement with Molnár (2011). This finding is consistent with the evidence that some myxozoans can infect closely related hosts (Forró and Eszterbauer, 2016).

5. Conclusion

The two morphologically similar spores, of *M. tharyensis* n. sp., from the European perch and *M. sandrae*, inhabiting the pikeperch and Volga pikeperch, could be merely differentiated by molecular data. The two species belong to phylogenetic sister groups and are the closest relatives of each other to date. The present study can serve as a basis for future studies confronted with a similar taxonomic complexity. It also supports the idea that appropriate molecular markers, in combination with morphological analysis, can play a crucial role in characterising the diversity of myxozoans.

Conflict of interest and authorship conformation form

Please check the following as appropriate.

All authors have participated in (a) conception and design, or analysis and interpretation of the data; (b) drafting the article or revising it critically for important intellectual content; and (c) approval of the final version.

This manuscript has not been submitted to, nor is under review at, another journal or other publishing venue.

The authors have no affiliation with any organization with a direct or indirect financial interest in the subject matter discussed in the manuscript

The following authors have affiliations with organizations with direct or indirect financial interest in the subject matter discussed in the manuscript:

Declaration of competing interest

The authors declare that they have no competing interests.

Acknowledgements

This study was funded by the Stipendium Hungaricum Program. We thank Gergely Zöldi for fish collection and maintenance, and Györgyi Pataki and Gregory Arjona Torres for the histological slides. Graciela Colunga-Ramírez is supported by CONAHCYT, Mexico (CVU 769732).

Appendix A. Supplementary data

Supplementary data to this article can be found online at <https://doi.org/10.1016/j.ijppaw.2024.100909>.

References

- Alama-Bermejo, G., Jirků, M., Kodádková, A., Pecková, H., Fiala, I., Holzer, A.S., 2016. Species complexes and phylogenetic lineages of *Hoferellus* (Myxozoa, Cnidaria) including revision of the genus: a problematic case for taxonomy. *Parasites Vectors* 9, 13. <https://doi.org/10.1186/s13071-015-1265-8>.
- Andree, K.B., Székely, C., Molnár, K., Gresoviac, S.J., Hedrick, R.P., 1999. Relationships among members of the genus *Myxobolus* (Myxozoa: bilvalvidae) based on small subunit ribosomal DNA sequences. *J. Parasitol.* 85, 68–74. <https://doi.org/10.2307/3285702>.
- Atkinson, S.D., Bartošová-Sojková, P., Whipps, C.M., Bartholomew, J.L., 2015. Approaches for characterising myxozoan species. In: Okamura, B., Gruhl, A., Bartholomew, J. (Eds.), *Myxozoan Evolution, Ecology and Development*. Springer, Cham. https://doi.org/10.1007/978-3-319-14753-6_6.
- Barta, J.R., Martin, D.S., Liberator, P.A., Dashkevich, M., Anderson, J.W., Feighner, S.D., Elbrecht, A., Perkins-Barrow, A., Jenkins, M.C., Danforth, H.D., Ruff, M.D., Profous-Juchelka, H., 1997. Phylogenetic relationships among eight *Eimeria* species infecting domestic fowl inferred using complete small subunit ribosomal DNA sequences. *J. Parasitol.* 83, 262–271. <https://doi.org/10.2307/3284453>.
- Bartošová-Sojková, P., Hrabcová, M., Pecková, H., Patra, S., Kodádková, A., Jurajda, P., Tým, T., Holzer, A.S., 2014. Hidden diversity and evolutionary trends in malacosporan parasites (Cnidaria: myxozoa) identified using molecular phylogenetics. *Int. J. Parasitol.* 44, 565–577. <https://doi.org/10.1016/j.ijpara.2014.04.005>.
- Bickford, D., Lohman, D.J., Sodhi, N.S., Ng, P.K.L., Meier, R., Winker, K., Ingram, K.K., Das, I., 2007. Cryptic species as a window on diversity and conservation. *Trends Ecol. Evol.* 22, 148–155. <https://doi.org/10.1016/j.tree.2006.11.004>.
- Brooks, D.R., Hoberg, E., 2000. Triage for the biosphere: the need and rationale for taxonomic inventories and phylogenetic studies of parasites. *Comp. Parasitol.* 67, 1–25.
- Castresana, J., 2000. Selection of conserved blocks from multiple alignments for their use in phylogenetic analysis. *Mol. Biol. Evol.* 17, 540–552. <https://doi.org/10.1093/oxfordjournals.molbev.a026334>.
- Cech, G., Molnár, K., Székely, C., 2012. Molecular genetic studies on morphologically indistinguishable *Myxobolus* spp. infecting cyprinid fishes, with the description of three new species, *M. alvarezae* sp. nov., *M. sijae* sp. nov. and *M. eirasianus* sp. nov. *Acta Parasitol.* 57, 354–366. <https://doi.org/10.2478/s11686-012-0045-2>.
- Cone, D.K., Anderson, R.C., 1977. Myxosporidian parasites of pumpkinseed (*Lepomis gibbosus* L.) from Ontario. *J. Parasitol.* 63, 657–666. <https://doi.org/10.2307/3279565>.
- Dallas, T.A., Becker, D.J., 2021. Taxonomic resolution affects host–parasite association model performance. *Parasitology* 148, 584–590. <https://doi.org/10.1017/S0031182020002371>.
- Darriba, D., Taboada, G.L., Doallo, R., Posada, D., 2012. jModelTest 2: more models, new heuristics and parallel computing. *Nat. Methods* 9, 772. <https://doi.org/10.1038/nmeth.2109>.
- Diamant, A., Whipps, C.M., Kent, M.L., 2004. A new species of *Sphaeromyxa* (Myxosporia: sphaeromyxina: Sphaeromyxidae) in devil firefish, *Pterois miles* (Scorpaenidae), from the northern Red Sea: morphology, ultrastructure and phylogeny. *J. Parasitol.* 90, 1434–1442. <https://doi.org/10.1645/GE-336R>.
- Eiras, J.C., Cruz, C.F., Saraiva, A., Adriano, E.A., 2021. Synopsis of the species of *Myxobolus* (Cnidaria, myxozoa, myxosporia) described between 2014 and 2020. *Folia Parasitol.* 68 <https://doi.org/10.14411/fp.2021.012>.
- Eszterbauer, E., 2002. Molecular biology can differentiate morphologically indistinguishable myxosporan species: *Myxobolus elegans* and *M. hungaricus*. *Acta Vet. Hung.* 50, 59–62. <https://doi.org/10.1556/avet.50.2002.1.8>.
- Ferguson, J.A., Atkinson, S.D., Whipps, C.M., Kent, M.L., 2008. Molecular and morphological analysis of *Myxobolus* spp. of salmonid fishes with the description of a new *Myxobolus* species. *J. Parasitol.* 94, 1322–1334. <https://doi.org/10.1645/GE-1606.1>.
- Forró, B., Eszterbauer, E., 2016. Correlation between host specificity and genetic diversity for the muscle-dwelling fish parasite *Myxobolus pseudodispar*: examples of myxozoan host-shift? *Folia Parasitol.* 63 <https://doi.org/10.14411/fp.2016.019>.
- Guo, Q., Huang, M., Liu, Y., Zhang, X., Gu, Z., 2018. Morphological plasticity in *Myxobolus* Bütschli, 1882: a taxonomic dilemma case and renaming of a parasite species of the common carp. *Parasites Vectors* 11, 399. <https://doi.org/10.1186/s13071-018-2943-0>.
- Hallett, S.L., Diamant, A., 2001. Ultrastructure and small-subunit ribosomal DNA sequence of *Henneguya lesteri* n. sp. (Myxosporia), a parasite of sand whiting *Sillago analis* (Sillaginidae) from the coast of Queensland, Australia. *Dis. Aquat. Org.* 46, 197–212. <https://doi.org/10.3354/dao046197>.
- Herrick, J.A., 1936. Two new species of *Myxobolus* from fishes of lake Erie. *Trans. Am. Microsc. Soc.* 55, 194–198. <https://doi.org/10.2307/3222611>.
- Holzer, A.S., Bartošová, P., Pecková, H., Tým, T., Atkinson, S., Bartholomew, J., Sípó, D., Eszterbauer, E., Dyková, I., 2013. 'Who's who' in renal sphaerosporids (Bivalvulida: myxozoa) from common carp, Prussian carp and goldfish – molecular identification of cryptic species, blood stages and new members of *Sphaerospora sensu stricto*. *Parasitology* 140, 46–60. <https://doi.org/10.1017/S0031182012001175>.
- Kottelat, M., Freyhof, J., 2007. *Handbook of European Freshwater Fishes*. Kottelat, Munich, Germany.
- Liu, Y., Lövy, A., Gu, Z., Fiala, I., 2019. Phylogeny of Myxobolidae (Myxozoa) and the evolution of myxospore appendages in the *Myxobolus* clade. *Int. J. Parasitol.* 49, 523–530. <https://doi.org/10.1016/j.ijpara.2019.02.009>.
- Lom, J., Arthur, J.R., 1989. A guideline for the preparation of species descriptions in Myxosporia. *J. Fish. Dis.* 12, 151–156. <https://doi.org/10.1111/j.1365-2761.1989.tb00287.x>.
- Lom, J., Pike, A.W., Dykova, I., 1991. *Myxobolus sandrae* Ruess, 1906, the agent of the vertebral column deformities of perch *Perca fluviatilis* in northeast Scotland. *Dis. Aquat. Org.* 12, 49–53.
- Milanin, T., Bartholomew, J.L., Atkinson, S.D., 2020. *Myxobolus* spp. (Cnidaria: Myxozoa) in introduced yellow perch *Perca flavescens* (Mitchill, 1814). *Parasitol. Res.* 119, 893–901. <https://doi.org/10.1007/s00436-019-06585-3>.
- Molnár, K., 1994. Comments on the host, organ and tissue specificity of fish myxosporans and on the types of their intrapiscine development. *Parasitol. Hung.* 27, 5–20.
- Molnár, K., 2011. Remarks to the validity of genbank sequences of *Myxobolus* spp. (myxozoa, myxosporidae) infecting eurasian fishes. *Versita* 56, 263–269. <https://doi.org/10.2478/s11686-011-0054-6>.
- Molnár, K., Eszterbauer, E., 2015. Specificity of infection sites in vertebrate hosts. In: Okamura, B., Gruhl, A., Bartholomew, J.L. (Eds.), *Myxozoan Evolution, Ecology and Development*. Springer International Publishing, pp. 295–313. https://doi.org/10.1007/978-3-319-14753-6_16.
- Molnár, K., Székely, C., 2014. Tissue preference of some myxobolids (Myxozoa: myxosporia) from the musculature of European freshwater fishes. *Dis. Aquat. Org.* 107, 191–198. <https://doi.org/10.3354/dao02688>.
- Rambaut, A., 2018. FigTree V. 1.4.4: Tree Figure Drawing Tool. <http://tree.bio.ed.ac.uk/software/figtree/>. (Accessed 10 August 2023).
- Ruess, H., 1906. Neue myxosporidien von Süßwasserfischen. *Bull. Scient. Acad. Imp. Sci. St. Petersburg.* 25, 199–205.
- Ronquist, F., Teslenko, M., Van Der Mark, P., Ayres, D.L., Darling, A., Höhna, S., Larget, B., Liu, L., Suchard, M.A., Huelsenbeck, J.P., 2012. MrBayes 3.2: efficient

- bayesian phylogenetic inference and model choice across large model space. *Syst. Biol.* 61, 539–542. <https://doi.org/10.1093/sysbio/sys029>.
- Sáez, A.G., Lozano, E., 2005. Body doubles. *Nature* 433 (7022), 111.
- Sellyei, B., Molnár, K., Czeglédi, I., Preiszner, B., Székely, C., 2022. Effect of 80% ethanol or 10% formalin fixation, freezing at 20 °C and staining on *Myxobolus* (Myxosporidia) spores to be deposited in parasitological collections. *Int. J. Parasitol. Parasites Wildl.* 19, 257. <https://doi.org/10.1016/j.ijppaw.2022.10.002>. –262.
- Specziár, A., Bfó, P., 2003. Population structure and feeding characteristics of Volga pikeperch, *Sander volgensis* (pisces, percidae), in Lake Balaton. *Hydrobiologia* 506, 503–510. <https://doi.org/10.1023/B:HYDR.0000008535.98144.1e>.
- Soltyńska, M., 1967. Myxosporidia of fishes from the zegrze lake. *Acta Protozool.* 4, 307–325.
- Székely, C., Borzák, R., Molnár, K., 2018. Description of *Henneguya jaczoi* sp. n. (Myxosporidia, myxobolidae) from *Perca fluviatilis* (L.) (Pisces, Percidae) with some remarks on the systematics of *Henneguya* spp. of European fishes. *Acta Vet. Hung.* 66, 426–443. <https://doi.org/10.1556/004.2018.038>.
- Talavera, G., Castresana, J., 2007. Improvement of phylogenies after removing divergent and ambiguously aligned blocks from protein sequence alignments. *Syst. Biol.* 56, 564–577. <https://doi.org/10.1080/10635150701472164>.
- Tamura, K., Stecher, G., Kumar, S., 2021. MEGA11: molecular evolutionary genetics analysis version 11. *Mol. Biol. Evol.* 38, 3022–3027.
- Vieira, D.H.M.D., Narciso, R.B., Da Silva, R.J., 2022. Morphological and molecular characterization of the cryptic species *Myxobolus cataractae* n. sp. (Cnidaria: myxozoa: Myxobolidae) parasitizing *Imparfinis mirini* (Siluriformes: heptapteridae). *Parasitol. Int.* 88, 102560 <https://doi.org/10.1016/j.parint.2022.102560>.
- Walsh, H.L., Blazer, V.S., Iwanowicz, L.R., Smith, G., 2012. A redescription of *Myxobolus inornatus* from young-of-the-year smallmouth bass (*Micropterus dolomieu*). *J. Parasitol.* 98 <https://doi.org/10.1645/GE-3081.1>, 1236–42.
- Wang, M., Zhang, J., Zhao, Y., 2022. Morphological description and molecular identification of *Myxobolus dajiangensis* n. sp. (Myxozoa: myxobolidae) from the gill of *Cyprinus carpio* in southwest China. *PeerJ* 10, e13023. <https://doi.org/10.7717/peerj.13023>.
- Wegener, G., 1910. *Die Ektoparasiten der Fische Ostpreussens* [Inaugural Dissertation]. Albertus University, Königsberg, p. 90.
- Weiperth, A., 2014. Effect of water level fluctuations on fishery and anglers' catch data of economically utilized fish species of Lake Balaton between 1901-2011. *Appl. Ecol. Environ. Res.* 12, 221–249. https://doi.org/10.15666/aeer/1201_221249.